

## Correlations between signals of the liquid-gas phase transition in nuclei

M. F. Rivet<sup>a</sup>, N. Le Neindre<sup>a</sup>, J. P. Wieleczko<sup>b</sup>, B. Borderie<sup>a</sup>, R. Bougault<sup>c</sup>, A. Chbihi<sup>b</sup>, J. D. Frankland<sup>b</sup>, M. Pârlog<sup>d\*</sup>, M. Pichon<sup>c</sup>, B. Tamain<sup>c</sup> and INDRA and ALADIN Collaborations

<sup>a</sup>Institut de Physique Nucléaire, F-91406 Orsay cedex, France

<sup>b</sup>GANIL, F-14076 Caen, France

<sup>c</sup>LPC, ENSICAEN et Université, F-14050 Caen, France

<sup>d</sup>NIPNE, RO-76900 Bucharest-Măgurele, Romania

Finite systems such as atomic nuclei present at phase transition specific features different from those observed at the thermodynamic limit. Several characteristic signals were found in samples of events resulting from heavy ion collisions at and above the Fermi energy. The concomitant observation of different signatures of a liquid-gas phase transition in nuclei on a given sample strongly supports the occurrence of this transition.

### 1. INTRODUCTION

A liquid-gas type phase transition is theoretically expected for nuclei owing to the analogy between the nucleon-nucleon interaction and the van der Waals force. Experimentally, indications of phase transition have been reported many years ago by groups studying multifragmentation. In the last few years progresses developed in the two domains: statistical physics built the concepts associated to the definition and signatures of phase transition in finite systems, among which atomic nuclei; on the experimental side new and performant  $4\pi$  multidetectors allowed to study carefully selected samples of events instead of working on singles data. Among those the INDRA array was used to detect charged products formed in a wide variety of nuclear collisions, which bring nuclei in a state where phase transition will occur. The quality of the exclusive measurements permitted to search for different signatures of the transition, as it seems obvious that the concomitant observation of several of them will strongly reinforce the hypothesis that a phase transition has occurred.

### 2. EXPERIMENTAL EVENT SAMPLES

The results presented in this contribution were obtained in experiments performed with the  $4\pi$  array INDRA operating at GANIL or at GSI and mostly concern systems, or sources, with about 200-230 nucleons: “fused sources” from Xe+Sn, Ni+Au reactions, Au

---

\*Present address: GANIL, F-14076 Caen, France

or Ta quasi-projectiles. In order to analyse data in the framework of statistical physics, one must select well defined sources. In central collisions this was done by two techniques: either a selection of compact sources by taking events whose main direction of emission deviates by more than  $60^\circ$  from the beam direction (Xe+Sn system) [1]; or for the asymmetrical Ni+Au system a discriminant analysis method [2]. In the case of “fused sources” the experimental distributions of excitation energy are narrow.

The selection is more delicate when one wants to isolate quasi-projectiles, because of the presence of direct and neck emissions. For symmetric systems, a first order separation is to identify as quasi-projectile (quasi-target) the ensemble of products with velocities parallel to the beam direction larger (smaller) than the centre of mass velocity. This method was used for the Au+Au data discussed later. The advantage of quasi-projectiles is that the whole possible range of excitation energy (0 - available energy) can be explored.

In all cases a tolerance of about 10% on the source charge is imposed.

Any of these data samples constitutes a statistical ensemble, in the sense of a collection of events with similar properties. To apply statistical physics analyses one must be careful about the correct framework (microcanonical, canonical ensembles, with or without dynamical constraints ... ).

### 3. SIGNALS OF PHASE TRANSITION : THEORETICAL BASES

While at the thermodynamic limit first order phase transitions are characterized by discontinuities or divergences of observables, smoother situations are expected in finite systems, which exhibit anomalous curvatures in thermodynamical potentials. Saying that the entropy,  $S(E)$ , presents a convex curvature at first order phase transition is fully equivalent to stating that the energy distribution is bimodal, meaning that at a given temperature correspond two different values of the energy. Another consequence is that, in a microcanonical framework, the caloric curve,  $T(E)$ , should present a backbending for the energy domain corresponding to the phase transition, and therefore the heat capacity,  $c=dE/dT$ , will have a negative branch. However caloric curves may differ depending on the thermodynamical path followed by the system in the temperature-pressure-energy space, and may not present any backbending, even at phase transition. A more robust signal was found in the fluctuations of the kinetic part of the energy, directly connected to the heat capacity: very large fluctuations sign a negative value of  $c$ . See [3,4] for reviews.

In this picture, one then expects to observe at the same time a bimodality of the energy and a negative heat capacity as signals of a first order phase transition in nuclei. Moreover as the system is then located in the mechanically unstable spinodal region of the phase diagram, additional information can be found in searching for characterization of the dynamics of the phase transition, which in nuclei may proceed through nucleation or spinodal decomposition. Many theoretical predictions being in favour of the latter [5], a third signal of phase transition might be the evidence of spinodal decomposition.

On another hand the first indications of phase transition in the nineties were related to critical behaviors, such as the observation of a power law mass distribution for light products of multifragmentation [6]. At the thermodynamic limit, scalings are general properties of matter near the critical point and thus typical of second order phase transitions. Recent studies have however shown that scaling properties were observed on a

much larger range when the considered system is finite: it is sufficient that the correlation length be close to the system size to observe scalings. In a lattice gas framework, for instance, it was demonstrated that Fisher scaling occurs when the system lies on a “critical line” which extends well inside the coexistence region [7]. *For nuclei scalings can therefore also be considered as indications of the occurrence of a first order phase transition.*

## 4. SIGNALS OF PHASE TRANSITION : EXPERIMENTAL EVIDENCES

Most of the data mentioned in this section are published, we will not illustrate them here but rather send the reader to the quoted references.

### 4.1. Dynamics of the phase transition: spinodal decomposition

Theoretical studies as well as semi-classical simulations of collisions showed that, in the course of the reaction, the system is driven to the spinodal region of the phase diagram [8,9]. If low enough densities are reached, the system will never recover to normal conditions, but rather break-up into pieces. The rupture is initiated by local density fluctuations which are amplified in an homogeneous way by the mean field, creating regular high density regions which will finally turn into equal size fragments, surrounded by nucleons and very small fragments (the gas). The signature of spinodal decomposition in infinite nuclear matter is thus the observation in the exit channel of fragments of a given size, linked to the wave length of the most unstable mode. Here again the picture is different for nuclei, because of their finiteness. Firstly in this case several modes have equal characteristic times, leading to fluctuations in the size and multiplicity of the fragments from event to event [8]. Beating of modes and coalescence during fragment separation may break the symmetry of each partition. And last, as fragments are born hot, the de-excitation stage also alters the partitions. As a result the favoured partitions resulting from spinodal decomposition of nuclei might only survive with a very small probability, making them difficult to reveal.

The method proposed to evidence enhanced equal-size fragment partitions uses higher order charge correlations [10], each event being characterized by the average and the standard deviation of its fragment ( $Z \geq 5$ ) charge distribution. The delicate point in any correlation function is the construction of uncorrelated events. The initial method did not account for charge conservation; the INDRA collaboration proposed two methods to remedy this drawback, which lead to different results. Applied to semi-classical simulations of collisions between Xe and Sn at 32A MeV, where it is known that spinodal decomposition does occur, the modified event mixing method did not show any print of favoured partitions [11], while the intrinsic probability method (IPM) enlightens an excess of about 1% of events where fragments have equal sizes. On experimental data the results of the two methods also differ, the event mixing method always leading to less positive conclusions. With the IPM, evidence of spinodal decomposition was found, at the level of 0.3-1% of the events, in central collisions between Xe and Sn at 32, 39 and 45A MeV, the signal vanishing at 50A MeV [12]. It appeared at 52A MeV for central Ni+Au collisions, but not at the lower energy of 32A MeV [13]. The thermal energy put in the systems showing prints of spinodal decomposition was evaluated (with the help of a statistical model) to 5-7A MeV [14].

## 4.2. Bimodality

By definition, at first order phase transition, the distribution of an order parameter, or of any related variable, should be bimodal in a canonical framework. This was looked for in Au quasi-projectiles from Au+Au collisions between 60 and 100A MeV. To mimic a canonical, or at least a gaussian ensemble [15], the sorting for the quasi-projectile was performed as a function of the transverse energy of the light charged particles (lcp,  $Z \leq 2$ ) emitted backward of the centre of mass,  $E_{t12}^{QT}$ . This is justified by the high efficiency of INDRA for lcp in the entire phase space. At first order  $E_{t12}^{QT}$  quantifies the dissipated energy. For a specific bin of  $E_{t12}^{QT}$  a bimodal distribution is found for the charge asymmetry of the two largest fragments of each event,  $(Z_{max} - Z_{max-1}) / (Z_{max} + Z_{max-1})$ , when plotted versus  $Z_{max}$ , see examples in fig. 2(a) and 2(b): two groups of events clearly stand out, large asymmetries correspond to a big fragment associated with one or several very small ones (residue, or liquid type), while asymmetries close to 0 are associated with events with more and smaller fragments (gas type). Outside this specific region, charge asymmetries are close to 1 for low  $E_{t12}^{QT}$ , and turn to 0 for high  $E_{t12}^{QT}$  [16].

In the transition  $E_{t12}^{QT}$  region, the properties of the two groups of events were investigated. The small asymmetry events have larger multiplicities of both fragments and lcp, indicating that the excitation energy of these events is larger than that of the other group. This is confirmed by calorimetry measurements: the energy distributions associated with the two groups of events are distinct, although overlapping [16]. If one admits that a selection of  $E_{t12}^{QT}$  fixes the temperature, then two values of the energy are correlated to it, which is the signature of a bimodal behaviour.

## 4.3. Negative heat capacities

The microcanonical heat capacity is a thermodynamic variable which has the specific property to present a negative branch in the transition zone for finite systems. Experimental determinations of the heat capacity rely on the measurements of kinetic energy fluctuations at freeze-out [3]. The heat capacity is given by the relation  $c = c_k^2 / (c_k - \langle A_0 > \times \sigma_k^2 / T^2)$ , where  $c_k = \delta \langle E_k / A_0 \rangle / \delta T$  is the kinetic heat capacity,  $A_0$  and  $T$  the mass and temperature of the system and  $\sigma_k$  the kinetic energy fluctuation. The heat capacity is negative when the fluctuation is larger than the reference kinetic heat capacity.

The method suffers however several drawbacks, some from lacks in the measured quantities (number and energy of neutrons, fragment masses), and others intrinsic to the method (reconstruction of the freeze-out configuration from the measured products). The influence of the implied hypotheses was carefully tested on event samples obtained in a statistical model, SMM [17]. Interestingly it was demonstrated that the method tends to decrease the fluctuations, meaning that large fluctuations, and thus negative heat capacities, are not an artefact created by the imperfections of the measurement.

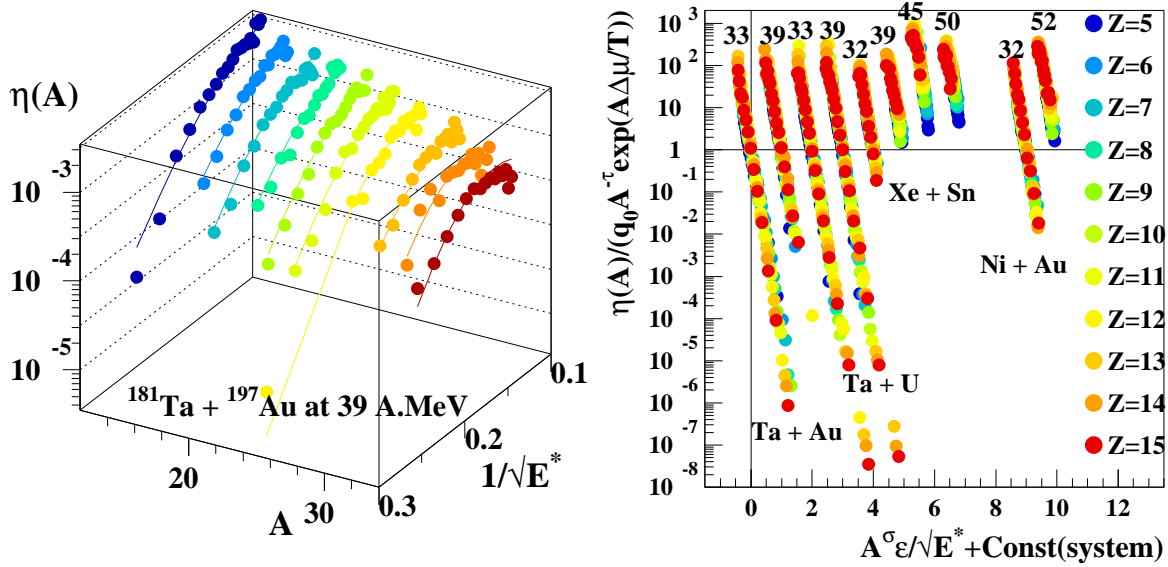
First observed on Au quasi-projectiles from 35A MeV Au+Au semi-peripheral collisions [18], negative heat capacities were also seen in INDRA data for the same reactions at 60-100A MeV incident energies [19]. The results of both experiments are in good agreement. In central collisions the end of the negative branch and the recovering to positive values were seen in Xe+Sn [20] and Ni+Au [13] collisions. The ranges of excitation energies where negative values of  $c$  were measured are in good enough agreement in all these cases, if one reminds that in central collisions some collective energy has to be added to

the potential energy part.

#### 4.4. Scalings

Two types of scalings were studied in the INDRA data. Fisher scaling was already found in many experiments, and critical exponents were extracted.  $\Delta$ -scaling was proposed more recently for determining the scenario of a second order phase transition.

##### 4.4.1. Fisher scaling



(a) Excitation functions for different nuclei produced in 39A MeV Ta+Au semi-peripheral collisions. Symbols are experimental data, lines show a fit with the Fisher formula.

(b) Scaled cross sections for nuclei from boron to phosphorus produced in semi-peripheral (Ta+X) or central (Xe+Sn, Ni+Au) collisions. Points for the different system, which all lie on a single curve, are shifted for a better view.

Figure 1. Fisher scaling

Fisher droplet model was originally proposed to study the morphology of fluids in thermal equilibrium in terms of an ideal gas of clusters coexisting with a liquid fraction. This model was recently applied to multifragmentation data, by considering all fragments but the largest as the gas phase,  $Z_{max}$  being assimilated to the liquid part. The yield of a fragment of mass  $A$  reads:  $dN/dA = \eta(A) = q_0 A^{-\tau} \exp((A\Delta\mu - c_0 \varepsilon A^\sigma)/T)$ . In this expression,  $\tau$  and  $\sigma$  are critical exponents,  $\Delta\mu$  is the difference between the chemical potentials of the two phases,  $c_0$  is the surface energy coefficient;  $\varepsilon = (T_c - T)/T_c$  describes the distance of the actual to the critical temperature. This kind of scaling was found in many multifragmentation data, in hadron-nucleus as well as in nucleus-nucleus collisions; the agreement between data and theory often holds over orders of magnitude, and the critical exponents which are deduced are in good agreement with those expected for the liquid-gas universality class. In INDRA data, Fisher scaling was applied to fragments obtained in single sources as well as in quasi-projectiles [21]. An example of the excitation functions for light fragments emitted by tantalum quasi-projectiles is given in fig. 1(a);

the Fisher formula well fits the experimental points over large ranges of masses and temperatures. Note that here the temperature is replaced by the square-root of the excitation energy, measured by calorimetry, according to the Fermi gas relation  $E^* = aT^2$ . In fig. 1(b) are shown the scaling properties of the data obtained for different fused systems (Xe+Sn, Ni+Au) or Ta quasi-projectiles from four different reactions; once scaled, all data collapse onto a single curve - they have been shifted along the abscissa on the figure for better visualisation. For quasi-projectiles, and for fused sources formed at 32A MeV, the scaling extends below and above the critical temperature. This unexpected behaviour comes from the finite size of the systems. As shown in [7], for finite systems the ‘‘Fisher critical temperature’’ obtained is not the true critical one if the system is in the coexistence region, and it varies with the density of the system. It happens for the data shown in fig. 1(b) that the critical excitation energies found are in all cases close to  $4.5A$  MeV [21]. If one remembers that the systems depicted in the figure also have similar masses, and thus may be represented by a single phase diagram, the unicity of the critical energy might be an indication that the density at phase transition (when the system multifragments) is similar for all systems, be they fused systems formed in violent collisions or quasi-projectiles from more peripheral collisions.

The values found for the topological exponent  $\tau$  (2.1-2.4) and the one related to the surface-volume dimensionality ratio  $\sigma$  (0.66) are in agreement with previous data, close to the ones of the liquid-gas universality class.

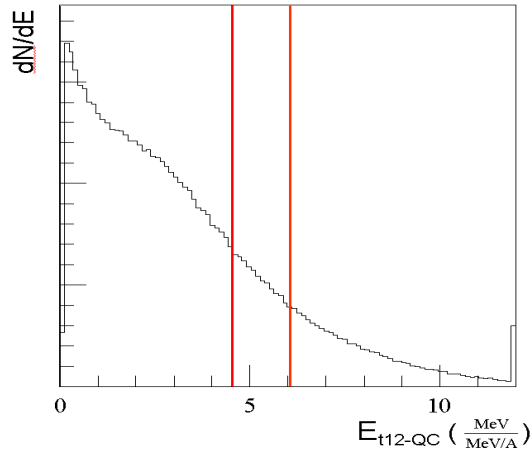
#### 4.4.2. Universal scaling

The theory of universal fluctuations of order parameters provides information on the relationship between the phase transition of a system and the formation of clusters, without requiring a precise knowledge of the thermodynamical state of this system [22]. All information is supposed to be contained in the multiplicity and size of the clusters. For systems which exhibit second-order critical behaviours, the critical order parameters can be identified through their  $\Delta$ -scaling behaviour.

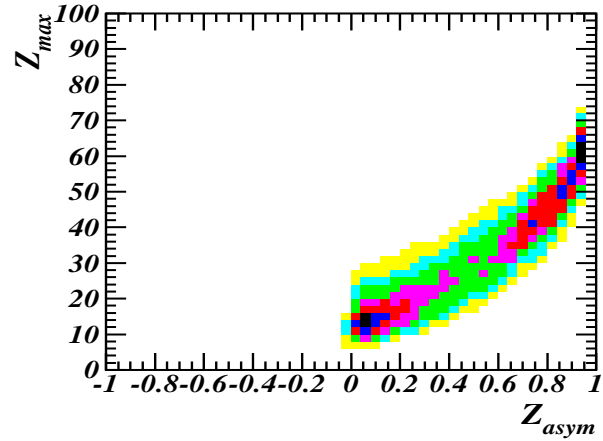
In the INDRA multifragmentation data on central collisions between a large variety of heavy ions, it appeared that the fragment multiplicity did not present any scaling, at variance with the size of the heaviest fragment,  $Z_{max}$ . The nature of the order parameter identifies multifragmentation as an aggregation scenario [23]. Symmetric systems with total masses between 73 and 394 all showed two scaling regimes, from  $\Delta=1/2$  at low incident energy to  $\Delta=1$  at higher energies, indicating the passage from an ordered phase to a disordered phase; the transition energy decreases when the systems grow heavier. (see [23,24] for details). It is interesting to note that the scaling behaviour is robust; for central collisions, it is rather independent of the precise event selection: the choice of compact sources [25] leads to  $Z_{max}$  distributions which are slightly narrower and shifted towards lower values than those obtained with an impact parameter selector [23], but the transition energy is barely displaced.

$\Delta$ -scaling was also evidenced in quasi-projectiles, provided that a selection is made via the bimodality order parameter. Events with large asymmetries scale with  $\Delta=1/2$  whereas those with more equal fragments scale with  $\Delta=1$ , see fig. 2(d).

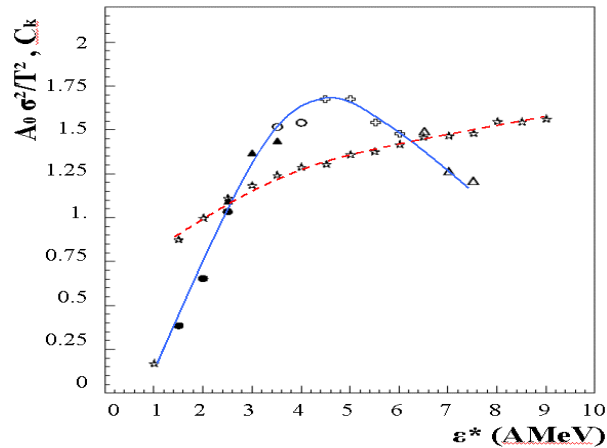
The  $\Delta$ -scaling signature of a phase transition is up to now the only one which has been observed without ambiguity for systems of total mass lighter than 150.



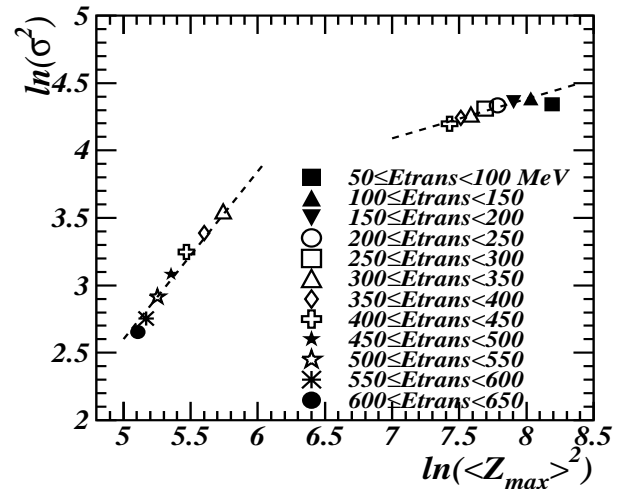
(a) Transverse energy distribution of lcp measured backward of the c.m. velocity, normalised to the incident energy per nucleon. The bars show the region where bimodality occurs.



(b) Charge of the largest fragment vs charge asymmetry of the two largest fragments,  $Z_{asym}$ .



(c) Kinetic heat capacity (stars, dotted line) and kinetic energy fluctuations (other symbols, full line.) Lines are to guide the eye.



(d)  $\Delta$ -scaling. Events with large charge asymmetry lie on the right branch ( $\Delta=1/2$ ), those with small asymmetry are on the left branch ( $\Delta=1$ ).

Figure 2. Quasi-projectiles from 80A MeV Au on Au collisions. Part (b) is obtained for events inside the bars in (a). See [16] for details. (from [19])

## 5. SIMULTANEOUS OBSERVATION OF SEVERAL SIGNALS

As said above, the hypothesis that atomic nuclei undergo a first order phase transition is strongly strengthened if several signatures of the transition are found on a given sample of events. Two examples will be presented in this section.

### 5.1. Quasi-projectiles from Au+Au reactions

The first case, shown in fig 2, is that of quasi-projectiles (QP) produced in Au+Au reactions at 80A MeV measured with INDRA at GSI. As explained in 4.2 the properties of quasi-projectiles were followed after sorting on  $E_{t12}^{QT}$ , the distribution of which is shown in fig. 2(a). Bimodality neatly occurs in the delimited  $E_{t12}^{QT}$  region, as shown in fig. 2(b).

The  $\Delta$ -scaling was searched for in all  $E_{t12}^{QT}$  bins, and appears when separating the two groups of events. Events associated with large asymmetries (or  $Z_{max}$ ) belong to the  $\Delta=1/2$  family, while those with small asymmetries correspond to  $\Delta=1$ : the transition is found in the energy region where bimodality occurs (diamonds and crosses in fig. 2(d)). Finally the negative heat capacity was calculated in a microcanonical framework inside each  $E_{t12}^{QT}$  bin. A further selection on event compactness was added for this study [19]. The excitation energy of quasi-projectiles is determined by calorimetry. In figure 2(c) are shown the kinetic energy fluctuations (solid line), versus the QP energy. Different symbols correspond to different bins of  $E_{t12}^{QT}$ . Fluctuations overcome the kinetic heat capacity (dotted line) in a small excitation energy domain of the QP (3-6A MeV), signing a negative value of the heat capacity; the largest fluctuations are obtained for events inside the  $E_{t12}^{QT}$  bin where bimodality occurs (crosses in fig. 2(c)). Note that fluctuations are maximum for an excitation energy of  $\sim 4.5A$  MeV, which is also the Fisher critical energy for similar (Ta) QP, as indicated in the previous section.

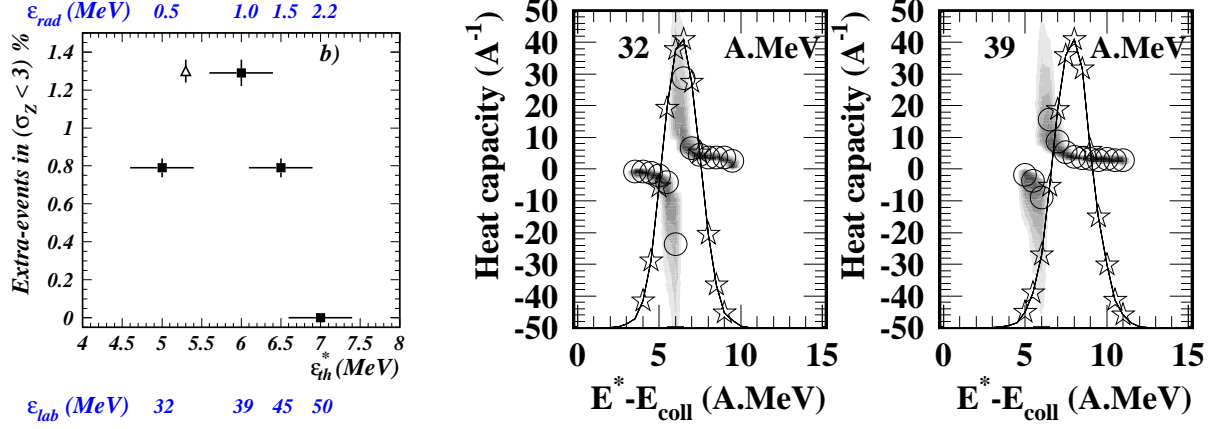
Finally, for the selected sample of Au quasi-projectiles excited at about 4-5A MeV two signals characteristic of a first order phase transition are found at the same time. The observation of a scaling law also supports the existence of such a transition, because the system studied is finite.

### 5.2. Single-source events from Xe+Sn reactions

The second example, displayed in fig 3, concerns fused sources formed in central xenon on tin collisions at 25, 32, 39, 45 and 50A MeV. The event samples are in all cases obtained with the same selection (compact event shapes). Fig 3(a) shows the excitation function of the excess of events with equal-sized fragments, signature of a spinodal decomposition. The trace of the phenomenon is maximum at 39A MeV. The end of the negative branch and the restoring to a positive value of the heat capacity are seen for the 32 and 39A MeV samples (fig. 3(b)). From the Fisher scaling one finds a critical excitation energy of 4.5A MeV, explored in the reaction at 32A MeV only; one expects a change in the multifragmentation pattern around this energy, which matches the energy where the kinetic energy fluctuations are maximum [21]. Finally the transition from order to disorder marked by the change in  $\Delta$  scaling also occurs between 32 and 39A MeV(fig. 3(d)).

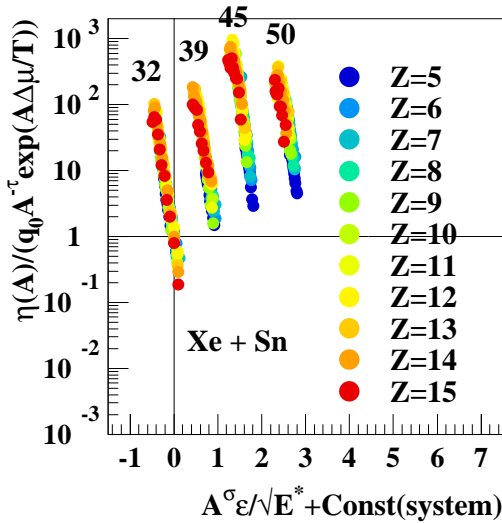
In summary, in events from central Xe on Sn collisions we have evidenced four signals indicating that the phase transition region is explored for incident energies between 32 and 39A MeV. The transition energies found in the different analyses do not fully coincide; calorimetry gives about 6A MeV, while a determination through a comparison with the SMM model indicates 5A MeV, close to the Fisher critical energy of 4.5A MeV. All values are however in agreement within the present precision of about 1A MeV that we have on calorimetry measurements.



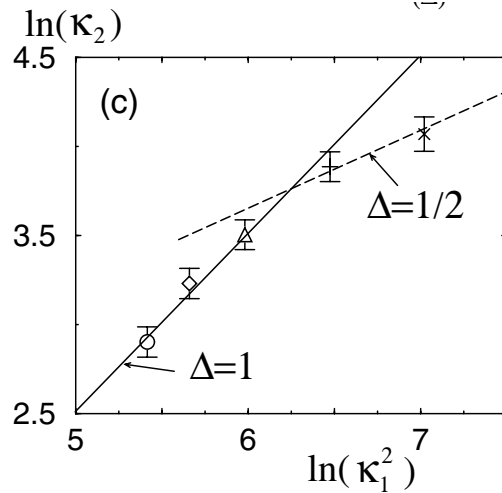


(a) Excitation function for the spinodal signal between 32 and 50A MeV (from [12]).

(b) Energy distribution and heat capacity for collisions at 32 and 39A MeV (from [17]).



(c) Fisher scaling at 32, 39, 45 and 50A MeV (from [21]).



(d)  $\Delta$ -scaling. Points from right to left were obtained for collisions at 25, 32, 39, 45 and 50A MeV. (from [25]).

Figure 3. Central collisions between Xe and Sn from 25 to 50A MeV

## 6. Summary and prospects

The two above examples clearly indicate that one can characterize a first order phase transition in nuclei with masses around 200, independently of the violence of the collision in which they were formed, and of the amount of radial expansion energy (larger in central than in peripheral collisions). Work is in progress to look for signatures of phase transition on lighter systems. To be more quantitative and do metrology, refinements of the methods are in progress, and experiments with larger statistical samples are necessary. In the future more information will be obtained when new accelerators will furnish very

exotic beams, permitting to explore the influence of the  $N/Z$  degree of freedom on phase transition. Calculations predict for instance the shrinking of the spinodal region when the number of neutron becomes very large [26]. Ultimately, reliable information should be gained on the symmetry term of the equation of state.

## REFERENCES

1. J. D. Frankland et al. (INDRA collaboration), Nucl. Phys. A 689 (2001) 905.
2. N. Bellaize et al. (INDRA collaboration), Nucl. Phys. A 709 (2002) 367.
3. P. Chomaz et al., T. Dauxois et al. (eds.) Dynamics and Thermodynamics of systems with long range interactions, Springer-Verlag, Heidelberg, 2002, vol. 602 of *Lecture Notes in Physics*, 68–129.
4. D. H. E. Gross, T. Dauxois et al. (eds.) Dynamics and Thermodynamics of systems with long range interactions, Springer-Verlag, Heidelberg, 2002, vol. 602 of *Lecture Notes in Physics*, 23–44.
5. P. Chomaz et al., Phys. Rep. 389 (2004) 263.
6. L. G. Moretto et al., G. Agnello et al. (eds.) Proc. Int. Workshop on Multifragmentation 2001, Catania, Italy, 2001, 33–48.
7. F. Gulminelli et al., Phys. Rev. Lett. 82 (1999) 1402.
8. B. Jacquot et al., Phys. Lett. B 383 (1996) 247.
9. A. Guarnera et al., Phys. Lett. B 403 (1997) 191.
10. L. G. Moretto et al., Phys. Rev. Lett. 77 (1996) 2634.
11. J. L. Charvet et al., Nucl. Phys. A 730 (2004) 431.
12. G. Tăbăcaru et al., Eur. Phys. J. A 18 (2003) 103.
13. B. Guiot, thèse de doctorat, Université de Caen (2002), <http://ccsd.cnrs.fr,tel-0003753>.
14. M. F. Rivet et al. (INDRA collaboration), G. Agnello et al. (eds.) Proc. Int. Workshop on Multifragmentation 2001, Catania, Italy, 2001, 11–20, nucl-ex/0205010.
15. M. Challa et al., Phys. Rev. Lett. 60 (1988) 77.
16. B. Tamain et al. (INDRA and ALADIN collaborations), this conference.
17. M. D’Agostino et al., Nucl. Phys. A 699 (2002) 795.
18. M. D’Agostino et al., Nucl. Phys. A 650 (1999) 329.
19. M. Pichon, thèse de doctorat, Université de Caen (2004).
20. N. Le Neindre, thèse de doctorat, Université de Caen (1999), <http://ccsd.cnrs.fr,tel-00003741>.
21. N. Le Neindre et al. (INDRA collaboration), I. Iori et al. (eds.) Proc. XL Int. Winter Meeting on Nuclear Physics, Bormio, Italy, Ricerca scientifica ed educazione permanente, 2002, 144.
22. R. Botet et al., Phys. Rev. E 62 (2000) 1825.
23. J. D. Frankland et al. (INDRA and ALADIN collaborations), Phys. Rev. C submitted, nucl-ex/0404024.
24. J. D. Frankland et al. (INDRA and ALADIN collaborations), this conference.
25. R. Botet et al., Phys. Rev. Lett. 86 (2001) 3514.
26. M. Colonna et al., Phys. Rev. Lett. 88 (2002) 122701.